

A phase diagram for spatio-temporal intermittency in the sine circle map lattice

Zahera Jabeen¹ and Neelima Gupte²

Abstract—

We study the phase diagram of the sine circle map lattice with random initial conditions and identify the various types of dynamical behaviour which appear here. We focus on the regions which show spatio-temporal intermittency and characterise the accompanying scaling behaviour. Directed percolation exponents are seen at some points in the parameter space in the neighbourhood of bifurcation boundaries. We discuss this behaviour as well as other types of behaviour seen in the parameter space in the context of the phase diagram.

Keywords— Coupled map lattice, Spatio-temporal intermittency.

I. INTRODUCTION

THE existence of spatio-temporal intermittency wherein laminar regions, which exhibit regular dynamics in space and time, co-exist and propagate together with regions which show irregular or chaotic bursts, which can be termed turbulent behaviour, can be seen in a wide variety of spatially extended systems. Examples of such systems range from oscillators, systems which show pattern formation [1], chemical reactions [2], to turbulence [3] and fluid flows [4], [5], [6]. The phenomenon of temporal intermittency has been studied extensively and is relatively well understood [7]. The nature of intermittency in spatially extended dynamical systems, however has not been understood very well. The presence of spatial as well as temporal intermittency has implications for understanding the physics of pattern formation and for understanding the ubiquitous presence of structures in chaotic systems.

Coupled map lattices, i.e. systems with continuous variables which evolve on discrete space-time, are particularly simple paradigms for systems with extended spatial dimension and show a wide range of interesting dynamical behaviour [1]. Spatio-temporal intermittency has been observed in a variety of coupled map lattices [8], [9], [10], [11]. Phase transitions to spatio-temporal intermittency are a topic of current interest, and the identification of the universality class of this transition has led to much discussion in the literature. Specifically, the type of spatio-temporal intermittency where there is no spontaneous creation of bursts, and a given laminar site can only become turbulent if infected by turbulent neighbours, has been conjectured to lie in the same universality class as directed percolation, with the laminar sites being identified as the ‘dry’ or absorbing states, and the turbulent sites being the ‘wet’ or percolating states. In another type of spatio-temporal intermittency, laminar sites can spontaneously become turbulent. These two types of intermittency have been called Type I and Type II spatio-temporal intermittency in the literature, respectively.

Recently, the existence of spatio-temporal intermittency has been observed at certain parameter values for the sine circle map lattice, a popular model for the behaviour of mode-locked oscil-

lators [11]. However, the detailed phase diagram of this model has not yet been obtained. In this paper we study the phase diagram of this model and identify the various types of dynamical behaviour which appear here. We next concentrate on the regions which show spatio-temporal intermittency and characterise the accompanying scaling behaviour. Directed percolation exponents are seen at some points in the parameter space in the neighbourhood of bifurcation boundaries. We discuss this behaviour as well as other classes of dynamical behaviour seen in the context of the bifurcation behaviour as well as the phase diagram of the system.

II. THE MODEL

In this paper, we consider the coupled circle map lattice [14] which has been used to model mode-locking behaviour. The coupled sine circle map lattice is defined by the evolution equations [12]:

$$x_{n+1}(i) = (1-\epsilon)f(x_n(i)) + \frac{\epsilon}{2}[f(x_n(i+1)) + f(x_n(i-1))](\text{mod } 1) \quad (1)$$

where t is the discrete time index, and i is the site index: $i = 1, \dots, L$, with L being the system size. The parameter ϵ gives the strength of the diffusive coupling between site i and its two neighbours. The local on-site map is given by

$$f(x) = x + \Omega - \frac{K}{2\pi} \sin(2\pi x) \quad (2)$$

where the parameter K is the strength of the nonlinearity, and Ω is the frequency of the single sine circle map in the absence of nonlinearity. This CML has been studied extensively and has a rich phase diagram with many types of attractors and strong sensitivity to initial conditions [12], [13]. In particular, this system also has regimes of spatio-temporal intermittency (STI) when evolved in parallel with random initial conditions [11]. For weak values of nonlinearity, i.e. for $K = 1.0$ the system shows spatio-temporal intermittency with a unique absorbing state at the parameter values $\Omega = 0.064$, $\epsilon = 0.63775$, and $\Omega = 0.068$, $\epsilon = 0.73277$. These mark the transition from a laminar phase to STI. The laminar phase here corresponds to the synchronised fixed point $x^* = \frac{1}{2\pi} \sin^{-1}(\frac{2\pi\Omega}{K})$, and the turbulent sites are those which are different from x^* . Spatio-temporal intermittency has also been observed for high values of nonlinearity $K = 3.1$, this time with infinitely many absorbing states. An earlier study of the inhomogeneous logistic map lattice had shown spatio-temporal intermittency in the neighbourhood of bifurcations from the synchronised fixed point of the system. It is therefore worthwhile to investigate the detailed phase-diagram of the present system, identify various types of dynamical behaviour, and correlate the observed behaviour, especially spatio-temporally intermittent behaviour, with the known bifurcations that occur in the system.

Both authors work at the Department of Physics, Indian Institute of Technology, Madras. We thank CSIR for partial financial support. e-mail: 1. zahera@physics.iitm.ac.in, 2. gupte@physics.iitm.ac.in

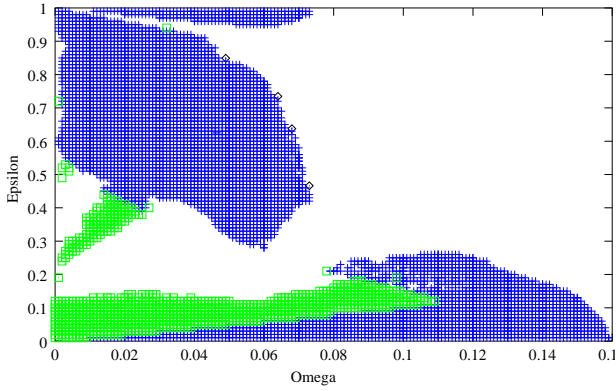


Fig. 1

The phase diagram in (ϵ, Ω) space for the coupled circle map lattice after 15000 iterations for a lattice of 1000 sites. Random initial conditions were used. The regimes of spatially synchronised and temporally fixed solutions (+) and the cluster solutions, where the number of clusters is less than 10 (\square) are shown. The points at which DP-like exponents are obtained are also marked (\diamond).

III. THE PHASE DIAGRAM

We study the system with random initial conditions at the parameter value $K = 1.0$ as detailed phase diagrams with other classes of initial conditions are available at this parameter value [12], [13], [14]. The single circle map shows temporal period 1 solutions in the region $0 \leq \Omega \leq \frac{1}{2\pi}$ and the coupled sine circle map shows synchronised, period 1 solutions over the same range when evolved with synchronised initial conditions [14]. There is a similar region between $1 - \frac{1}{2\pi} \leq 1$. We investigate this region for $0 \leq \epsilon \leq 1$ with random initial conditions. The phase diagram for this region can be seen in Fig. 1. The following types of dynamical behaviour can be found here.

1. Synchronised solutions: These constitute the dominant behaviour over the bulk of the parameter space and are very stable to perturbation. These are indicated by plus signs in Fig. 1.
2. Cluster solutions: There are regions which correspond to clusters where the variables on the lattice take up a finite number of values, but at random sites in the lattice. e.g. a 2-cluster is a solution where the lattice variables take up only two values, and sites which have the same value for the variable, belong to the same cluster. Regions which have less than 10 clusters are indicated by boxes in the phase diagram.
3. Spatio-temporally intermittent solutions can be seen at the parameter values marked with diamonds in this region. We discuss these solutions in detail in the next section.
4. Spatio-temporally disordered solutions can be seen in the white regions in the parameter space.

It is clear that the synchronised solutions change to cluster solutions at some of the phase boundaries, and to spatio-temporally disordered regions at others. There are some regions where a partially ordered phase is seen in the phase diagram where there are many clusters. The boundary between this partially ordered phase and the spatio-temporally disordered phase is not clear. While there are various interesting aspects to the behaviour of the cluster solutions, we will concentrate on the behaviour of the spatio-temporally intermittent solutions in this

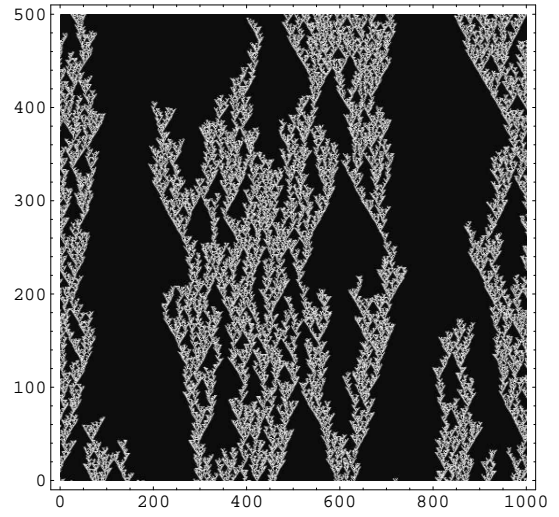


Fig. 2

A space-time plot for the spatio-temporal intermittency seen in the coupled circle map lattice at $\Omega = 0.049$, $\epsilon = 0.8495$. Horizontal axis is space and time is along the vertical axis. The system size chosen is $L = 1000$ and 15000 iterations have been discarded. The black region corresponds to the laminar state and the white region corresponds to the turbulent state. Every 10^{th} iterate has been plotted.

paper.

IV. SPATIO-TEMPORAL INTERMITTENCY AND DIRECTED PERCOLATION EXPONENTS

Spatio-temporally intermittent regions can be seen at several points in the parameter space. The points at which spatio-temporal intermittency of the first type are seen are marked on the phase diagram. As mentioned earlier, $\Omega = 0.064$, $\epsilon = 0.63775$, and $\Omega = 0.068$, $\epsilon = 0.73277$ are two of these points with a unique absorbing state with the value $x^* = \frac{1}{2\pi} \sin^{-1}(\frac{2\pi\Omega}{K})$. The same kind of spatio-temporally intermittent behaviour is found at two more points in the parameter space viz. $\Omega = 0.049$, $\epsilon = 0.8494$ and $\Omega = 0.073$, $\epsilon = 0.4664$. To verify whether the spatio-temporal intermittency here belongs to the universality class of directed percolation, set of critical exponents which describe the scaling behaviour of the quantities of physical interest have been calculated. The physical quantities of interest for such systems are (a) the escape time τ , which is the number of time steps elapsed before the system reaches its laminar state and (b) the order parameter, $m(\epsilon, L, t)$, which is the fraction of turbulent sites in the lattice at time t . From finite-size scaling arguments, it is expected that τ depends on L such that

$$\tau(\Omega, \epsilon) = \begin{cases} \log L & \text{laminar phase} \\ L^z & \text{critical phase} \\ \exp L^c & \text{turbulent phase} \end{cases}$$

Here, c is a constant of order unity, and the critical point is identified as the set of parameter values at which τ shows power-law behaviour with z being the critical exponent. At ϵ_c the critical value of the parameter ϵ (other parameters being held fixed), the

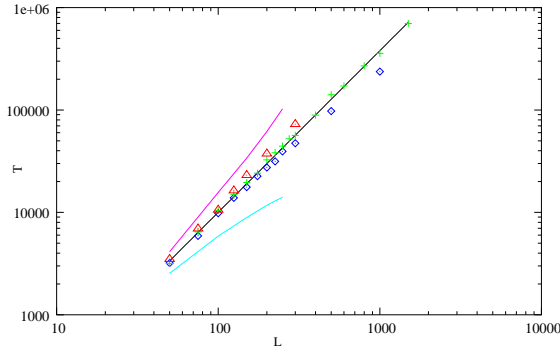


Fig. 3

The escape time, τ vs the system size, L is plotted at ϵ values below, at and above criticality at $\Omega = 0.049$ on a log – log scale. The values of ϵ plotted are 0.845, 0.849, 0.8494, 0.85, 0.852. Power law behaviour is seen at $\epsilon_c = 0.8494(+)$. The data at ϵ_c is fitted to an exponent 1.578.

order parameter $m(\epsilon, L, t)$ scales as

$$m \sim (\epsilon - \epsilon_c)^\beta, \quad \epsilon \rightarrow \epsilon_c^+. \quad (3)$$

when the critical line is approached from above .

The order parameter is expected to obey the scaling relation

$$m(\epsilon_c, L, t) \approx t^{-\beta/\nu z} \quad (4)$$

for $t \ll \tau$. The exponent ν can thus be extracted once β and z are obtained from the relations above.

To extract further critical exponents, we obtain the correlations from the pair correlation function given by:

$$C_j(t) = \frac{1}{L} \sum_{i=1}^L \langle x_i(t)x_{i+j}(t) \rangle - \langle x_i(t) \rangle^2 \quad (5)$$

where the brackets denote the averaging over different initial conditions. At criticality one expects an algebraic decay of correlation [15]:

$$C_j(t) \approx j^{1-\eta'}$$

where η' is the associated critical exponent.

The above set of exponents constitute the static exponents of the model. The dynamic exponents are given by the spreading exponents defined as follows. We consider temporal evolution from initial conditions which correspond to an absorbing background with a localised disturbance, i.e. a few contiguous sites which are different from an absorbing background. The quantities of interest are, the time dependence of $N(t)$, the number of active sites at time t averaged over all runs, $P(t)$, the survival probability, or the fraction of initial conditions which show a non-zero number of active sites (or a propagating disturbance) at time t and the radius of gyration $R^2(t)$, which is defined as the mean squared deviation of position of the active sites from the original sites of the turbulent activity, averaged over the surviving runs alone. At criticality, we have,

$$N(t) \approx t^\eta, \quad P(t) \approx t^{-\delta}, \quad R^2(t) \approx t^{z_s}.$$

Also, $\delta = \beta/\nu z$.

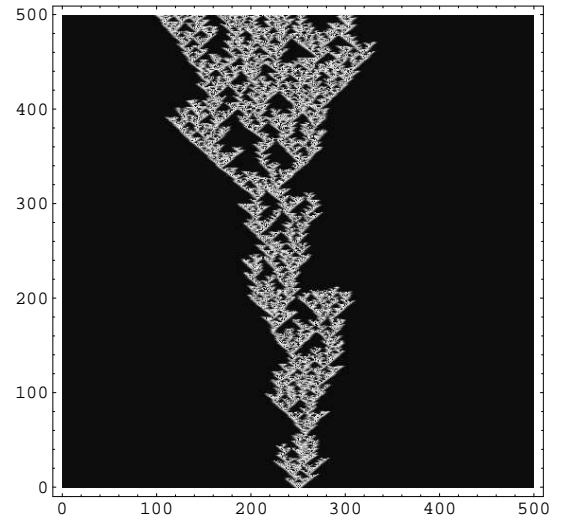


Fig. 4

We show the spreading of turbulent (white) sites in a laminar (black) background with 2 initial seeds. The horizontal axis is space and time is along the vertical axis. $\Omega = 0.049$, $\epsilon = 0.8494$. Lattice size, $L = 500$. Every 10^{th} iterate has been plotted.

The computed values for all the exponents above defined at the critical values $\Omega = 0.049$, $\epsilon = 0.8494$ and $\Omega = 0.073$, $\epsilon = 0.4664$ are listed in Table I. It is clear that the calculated exponents agree very well with the exponents for directed percolation. Thus the spatio-temporal intermittency at the points indicated by crosses in the phase diagram (Fig.1) belongs convincingly to the directed percolation class.

TABLE I

This table compares static CML exponents with the static DP exponents

Ω	ϵ	z	$\beta/\nu z$	β	ν	η'
0.049	0.8494	1.578	0.16	0.278	1.1	1.51
0.073	0.4664	1.58	0.16	0.278	1.1	1.515
DP		1.58	0.16	0.28	1.1	1.51

TABLE II

This table compares dynamic CML exponents with the dynamic DP exponents

Ω	ϵ	η	δ	z_s
0.049	0.8494	0.313	0.16	1.26
0.073	0.4664	0.313	0.16	1.26
DP		0.313	0.16	1.26

V. DISCUSSION

It is interesting to note that the parameter values which correspond to spatio-temporal intermittency all lie close to the bifurcation boundaries where bifurcations from synchronised solutions take place. The uppermost point where spatio-temporal intermittency is seen corresponds to a tangent-period doubling bifurcation, where two eigen-values of the stability matrix cross +1 and -1 respectively, whereas a tangent-tangent bifurcation

where several of the eigen values cross the unit circle takes place at the other values. The synchronised solutions go to spatio-temporally chaotic solutions via spatio-temporal intermittency at these values, whereas they go to spatio-temporal chaos via cluster solutions in other places. Spatio-temporal intermittency can also be seen at other locations in the phase diagram. The exact nature of this behaviour is presently under investigation. We also hope to look at these and other aspects of dynamical behaviour in further detail in future work.

REFERENCES

- [1] *Theory and Applications of Coupled Map Lattices*, edited by K. Kaneko (John Wiley, England, 1993) and references therein.
- [2] R.Kapral in *Theory and Applications of Coupled Map Lattices*, edited by K.Kaneko, John Wiley 1993 and references therein.
- [3] *Dynamical systems Approach to turbulence* by T. Bohr, M.H. Jensen, G. Paladin and A. Vulpiani, Cambridge University Press, (1998).
- [4] *Turbulent bursting and spatiotemporal intermittency in the counter rotating Taylor-Couette system*, G. Colovas and C. David Andereck, Phys.Rev.E **55**(3) 2736 (1997).
- [5] *Spatiotemporal Intermittency in Rayleigh-Benard Convection*, S. Ciliberto and P. Bigazzi, Phys.Rev.Lett.**60**, 286 (1988)
- [6] *Transition to weak turbulence via spatiotemporal intermittency in the Taylor-Dean system*, M.M. Degen, I. Mutabazi and C.D. Andereck, Phys.Rev. E**53** 3495 (1996).
- [7] P. Berge, Y. Pomeau and C. Vidal, *Order and Chaos in Nonlinear Systems*, John Wiley 1982.
- [8] *Transition to turbulence via spatio-temporal intermittency*, H.Chate and P.Manneville, Phys. Rev. Lett **58** 112 (1987). H.Chate, Europhys.Lett. **21** 419(1993).
- [9] *Breakdown of Universality in Transitions to Spatiotemporal Chaos*, T. Bohr, M. van Hecke, R. Mikkelson and M. Ipsen, Phys. Rev. Lett., **86**, 5482 (2001).
- [10] *Phase transitions in coupled map lattices*, P. Grassberger and T. Schreiber, Physica D **50**, 177 (1991).
- [11] *Evidence for directed percolation universality at the onset of spatiotemporal intermittency in coupled circle maps*, T.M. Janaki, S. Sinha and N. Gupte, Phys. Rev. E **67**, 056218 (2003).
- [12] *Mode locking of spatiotemporally periodic orbits in coupled sine circle map lattices*, G.R. Pradhan, N. Chatterjee and N. Gupte, Phys. Rev. E **65**, 046227 (2002).
- [13] *New characterisers of bifurcations from kink solutions in a coupled sine circle map lattice*, G.R. Pradhan and N. Gupte, Int. J. Bifurcations and Chaos, **11**, 2501, (2001).
- [14] *Synchronization in coupled sine circle maps*, N. Chatterjee and N. Gupte, Phys. Rev. E, **53**, 4457 (1996).
- [15] *Critical correlations in coupled map lattices*, J.M. Houlrik and M.H. Jensen, Phys. Lett. A **163**, 275 (1992).